P6.13 GLOBAL AND MONTHLY DIURNAL PRECIPITATION STATISTICS BASED ON PASSIVE MICROWAVE OBSERVATIONS FROM AMSU

Frederick W. Chen*, David H. Staelin, and Chinnawat Surussavadee
Massachusetts Institute of Technology, Research Laboratory of Electronics
Cambridge, Massachusetts

1. ABSTRACT

This paper presents climatological studies of precipitation-rate estimates based on data from the Advanced Microwave Sounding Unit instruments, AMSU-A and AMSU-B, aboard the NOAA-15, NOAA-16, and NOAA-17 satellites; and the corresponding set of instruments, AMSU and the Humidity Sounder for Brazil (HSB), aboard the NASA Aqua satellite. A precipitation-rate retrieval algorithm for these instruments has been developed (Chen and Staelin, IEEE Trans. Geosci. & Remote Sensing, 41(2)). This algorithm relies primarily on the opaque microwave bands near 54 and 183.31 GHz, which correspond to oxygen and water vapor absorption bands, respectively, and are particularly sensitive to glaciated precipitation. Most prior efforts towards satellite-based passive microwave remote sensing of precipitation (e.g. using TMI, SSM/I, and AMSR-E data) have relied primarily on window channels. The AMSU algorithm has shown promising agreement with NEXRAD over the eastern U.S. and plausible results globally. The NOAA-15, NOAA-16, and NOAA-17 satellites are polar-orbiting with equatorial crossing times of approximately 7 AM/PM, 2 AM/PM, and 10 AM/PM, respectively. The AMSU-A/B's aboard these satellites are able to observe each point on the globe approximately six times a day, and the sun-synchronous positioning permits meaningful study of the diurnal variations of glaciated precipitation. Maps of climatological statistics such as rain averages, rain frequencies, diurnal variations based on rain averages, and diurnal variations based on rain frequency will be presented for the period from June 2002 to January 2004.

2. INTRODUCTION

Precipitation climatology is important to hydrology and the study of the global energy cycle. This paper presents a global precipitation climatology study based on data from the Advanced Microwave Sounding Unit (AMSU) aboard the National Oceanographic and Atmospheric Administration (NOAA) NOAA-15, NOAA-16, and NOAA-17 satellites. Mean rain rates, rain frequencies, and diurnal cycles for monthly, seasonal, and yearly time scales are presented.

Global precipitation climatology has many significant modes of variation, one being the diurnal cycle which has not been thoroughly studied. A comprehensive study of the diurnal variations of precipitation over the continental U.S. was done by Dai et al. (1999). Satellite-based studies include those by Chang et al. (1995) using data from the Special Sounder Microwave Imager (SSM/I) data, and by Negri et al. (2002) using data from the Tropical Rainfall Measurement Mission (TRMM) Microwave Imager (TMI).

3. DESCRIPTION OF AMSU

AMSU is a passive microwave instrument with channels in the opaque 54-GHz oxygen and 183-GHz water vapor resonance bands; it also includes some window channels near 23.8, 31.4, 89, and 150 GHz. AMSU's are aboard the NOAA-15, -16, and -17 polar-orbiting satellites, which were launched in 1998, 2000, and 2002, respectively. These three satellites have local equatorial crossing times that are separated by ~3-5 hours. AMSU/HSB aboard the Aqua satellite (launched in 2002) provided a nearly identical set of channels. These four satellites observed each point on the globe ~8 times daily for a period of about seven months and at least two are expected to operate into the future.

4. THE PRECIPITATION RETRIEVAL ALGORITHM

Chen and Staelin have developed a method for estimating precipitation rate using opaque channels together with window channels (Chen and Staelin, 2003; Staelin and Chen, 2000). While previous satellite-based methods have relied exclusively on window channels, opaque channels are useful because they are insensitive to surface

* *Corresponding author address*: Frederick W. Chen, 77 Massachusetts Ave., Room 26-344, Cambridge, MA 02139; e-mail: fwchen@jansky.mit.edu

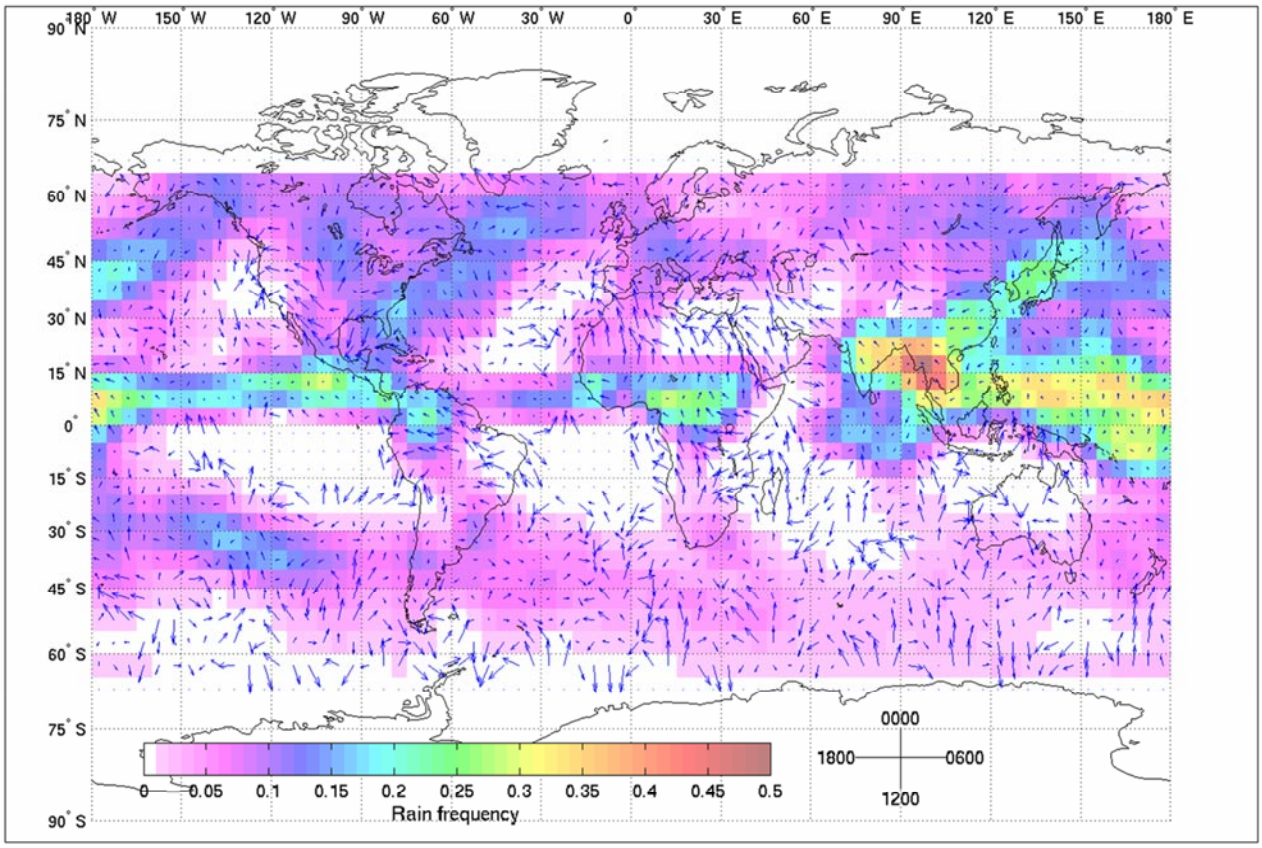

Fig. 1. Diurnal variations of rain frequency for Aug. 2002. Lengths of arrows represent mean-normalized diurnal amplitudes up to 0.5. Directions of arrows represent preferred local times of precipitation.

variations and they are sensitive to humidity, grauple size, and cloud-top altitude, which are important determinants of precipitation. This algorithm was trained using NEXRAD data over the eastern U.S. and adjusted using data from the Advanced Microwave Sounding Radiometer for the Earth Observing System (AMSR-E) aboard the NASA Aqua satellite (Chen, 2004).

One weakness of the algorithm is that it does not detect warm rain. The algorithm was developed primarily for convective precipitation.

In addition to rain, AMSU also has been shown to be useful for estimating snow (Chen, 2004; Chen and Staelin, 2003; Chen et al., May 2003; Chen et al., July 2003; Skofronick-Jackson et al., 2004).

5. COMPUTATION OF DIURNAL CYCLE

This section describes the model of the diurnal cycle and the computation of its parameters. Let R be the mean rain rate or rain frequency over a specified period (e.g. a month, a season, a year) as a function of the time of day t in hours. $R(t)$ is assumed to have the following form:

$$R(t) = A\cos[\omega(t-\tau)] + c \qquad (1)$$

where A is the non-negative diurnal amplitude, c the mean of $R(t)$, ω is the angular frequency of the diurnal cycle, and τ is the preferred time of precipitation. Since t is in hours, $\omega = \pi/24$. $R(t)$ can be rewritten as follows:

$$R(t) = a\cos(\omega t) + b\sin(\omega t) + c \qquad (2)$$

where $a = A\cos(\omega\tau)$ and $b = A\sin(\omega\tau)$. Then, with the six daily observations provided by the NOAA-15, NOAA-16, and NOAA-17 satellites, one can use least-squares approximation to determine the three unknowns, a, b, and c. a and b can then be used to compute A and τ. This method was used also by Chang et al. (1995).

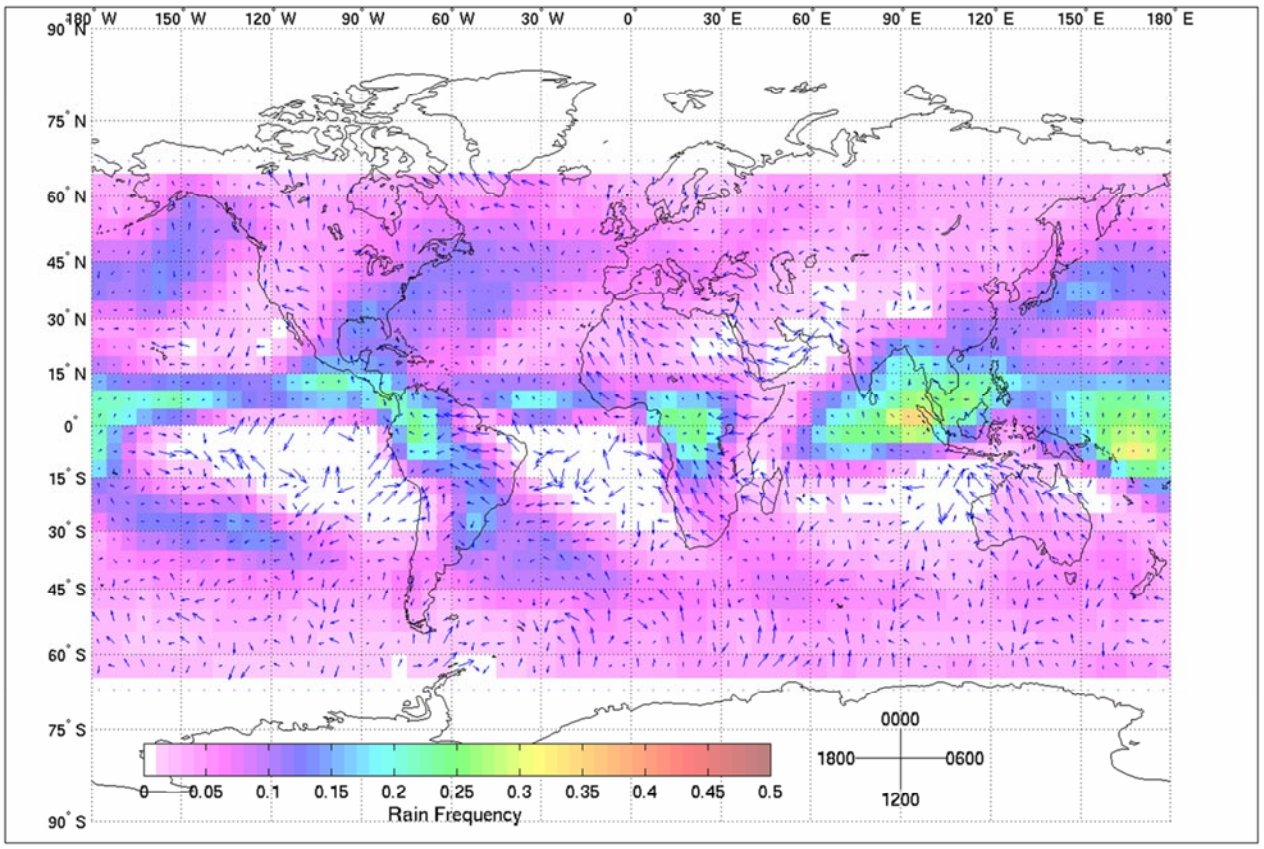

Fig. 2. Diurnal variations of rain frequency from Sept. to Nov. 2002. Lengths of arrows represent mean-normalized diurnal amplitudes up to 0.5. Directions of arrows represent preferred local times of precipitation.

6. SAMPLES OF CLIMATOLOGICAL RESULTS

Diurnal variations were computed for a 5°×5° latitude-longitude grid with mean rain rate and rain frequencies computed over 10°×10° boxes. Each diurnal cycle map has (1) a faded background image representing the mean rain rate or rain frequency, and (2) a quiver plot with arrows whose length and direction represent the mean-normalized diurnal amplitude and the preferred time of precipitation, respectively.

6.1 *1-Month Diurnal Cycle of Rain Frequency*

Fig. 1 shows the diurnal variations of rain frequency for Aug. 2002. It is clear that there is some systematic geographical variation. For example, over northern Africa, the preferred times of precipitation tend to be between 1900 and 0000. However, the noise in the quiver plot suggests that studies using 1-month-10°×10° space-time averages will yield a limited amount of information.

6.2 *Interseasonal Comparison of the Diurnal Cycle of Rain Frequency*

Figs. 2-4 show seasonal diurnal variations of rain frequency for four seasons. Over northern Africa, where there is strong diurnal character, the preferred time of precipitation is approximately 2100, 0100, and 2300, for the periods Sept. to Nov. 2002, Dec. 2002 to Feb. 2003, and March to May 2003, respectively. This shows a systematic seasonal variation in the diurnal cycle. These figures also show less noise in the quiver plot than Fig. 1.

6.3 *1-Year Diurnal Cycle of Rain Frequency*

Fig. 5 shows the diurnal cycle of rain frequency from July 2002 to June 2003 based on NOAA-15, NOAA-16, and NOAA-17 data from AMSU-A/B. The direction and length of the arrows seem to vary rather smoothly over most of the area between 65° N and 65° S. Strong diurnal character is evident over dryer regions such as northern Africa, northern Australia, and the western U.S. Over these regions, the preferred

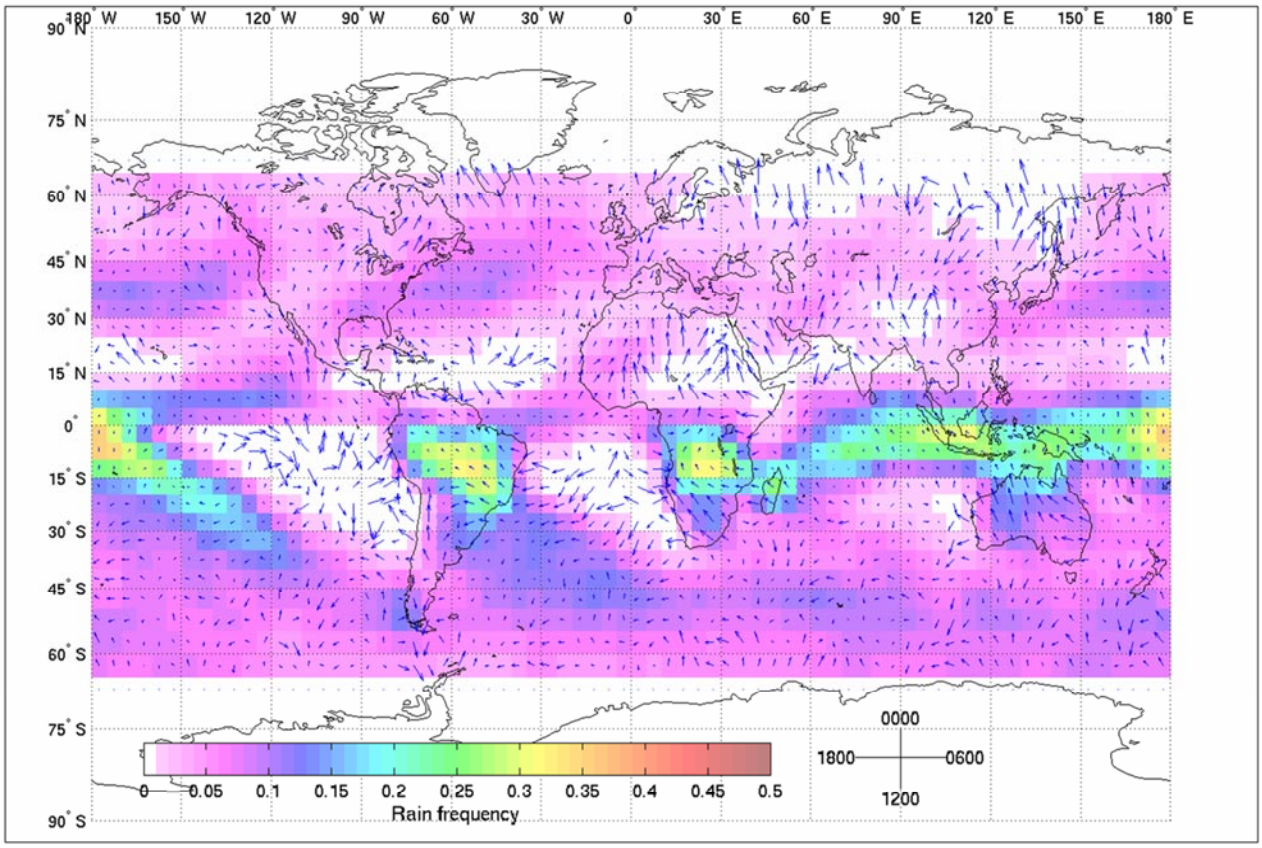

Fig. 3. Diurnal variations of rain frequency from Dec. 2002 to Feb. 2003. Lengths of arrows represent mean-normalized diurnal amplitudes up to 0.5. Directions of arrows represent preferred local times of precipitation.

times of precipitation are around 2200, 2200, and 2100 UTC, respectively. The mean-normalized diurnal amplitude and preferred time of precipitation also seems to vary smoothly over northern South America where the rain frequency is higher than in most other locations. The results for the period July 2001 to June 2002 were generally consistent with the results in Fig. 5 despite the fact that from this period only two satellites were used in the computation while three were used for Fig. 5. Also, it is not surprising that the direction and length of the arrows seems random in the white regions where the rain frequency is less than 1%.

6.4 *1-Year Diurnal Cycle of Rain Rate*

Fig. 6 shows the diurnal cycle of rain rate from July 2002 to June 2003 based on NOAA-15, NOAA-16, and NOAA-17 data from AMSU-A/B. Like Figs. 2-5, Fig. 6 shows systematic geographical variations. However, the quiver plot shows more random noise which is not surprising since rain frequency is an average of binary random variables while rain rate can have a lognormal distribution. There is a significant degree of correlation between Figs. 5 and 6. Over northern Africa, northern Australia, and the western U.S., the preferred times of precipitation based on mean rain rates and rain frequencies are nearly equal. However, there are regions where that it not so. Over northern South America, the preferred times of precipitation based on rain frequency is about 2000 while those based on mean rain rates varies between 2200 and 0100.

7. ACKNOWLEDGEMENTS

This work was sponsored by the National Aeronautics and Space Administration under contract NAS5-31376 and grant NAG5-13652.

8. REFERENCES

Chang, A.T.C., L.S. Chiu, and G. Yang, 1995: Diurnal Cycle of Oceanic Precipitation from SSM/I Data. *Monthly Weather Review*, **123**, 3371-3380.

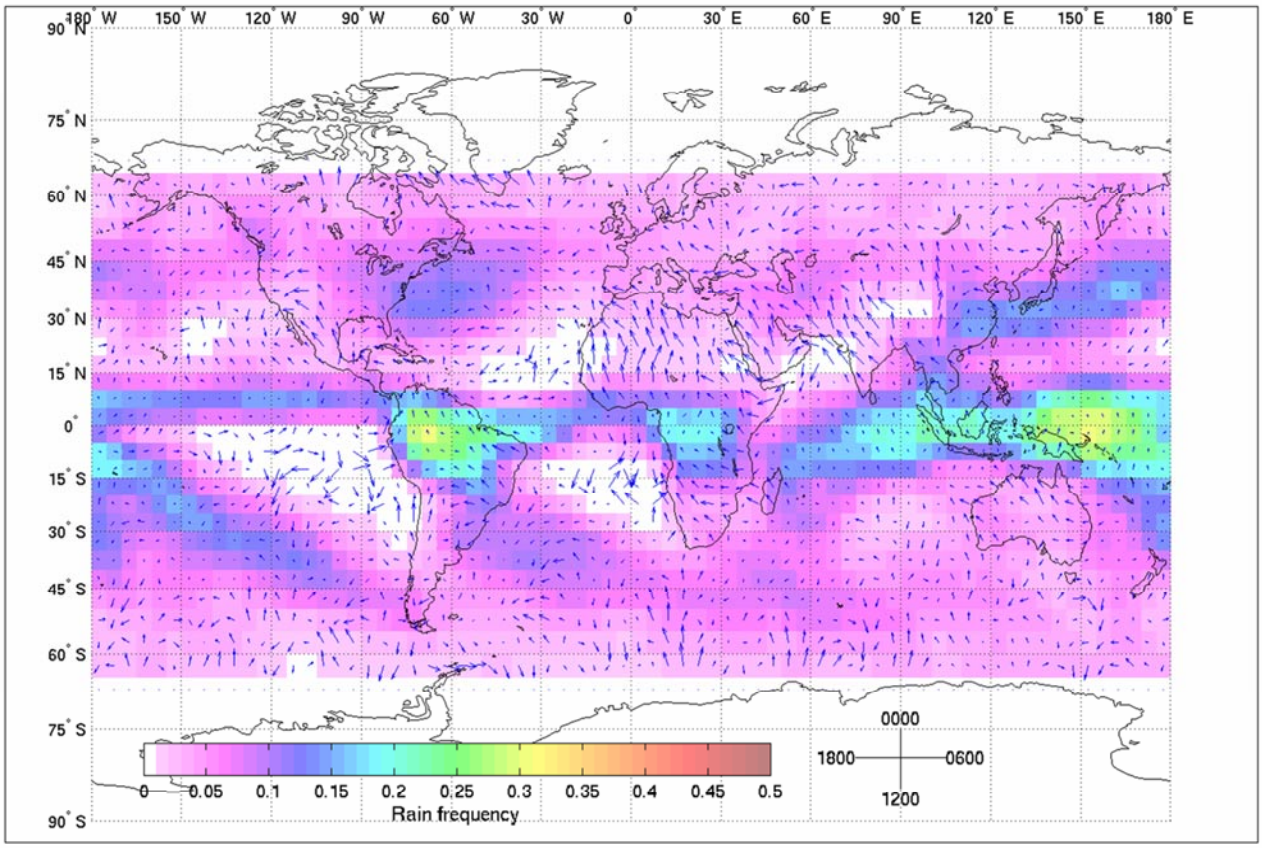

Fig. 4. Diurnal variations of rain frequency from Mar. 2003 to May 2003. Lengths of arrows represent mean-normalized diurnal amplitudes up to 0.5. Directions of arrows represent preferred local times of precipitation.

Chen, F.W. and D.H. Staelin, 2003: AIRS/AMSU/HSB Precipitation Estimates, *IEEE Trans. Geoscience and Remote Sensing*, **41**, 410-417.

Chen, F.W., A.M. Leckman, and D.H. Staelin, 2003: Satellite Observations of Polar Precipitation Using Aqua, *7th Conference on Polar Meteorology and Oceanography and Joint Symposium on High-Latitude Climate Variations*, Hyannis, MA, American Meteorological Society (available at <http://ams.confex.com/ams/7POLAR/7POLARCLIM/>).

Chen, F.W. and D.H. Staelin, July 2003: Passive Microwave Signatures of Arctic Snowstorms Observed from Satellites, *Proc. 2003 IEEE Int'l Geosci. Remote Sensing Symp.*, Toulouse, France, IEEE, **5**, 3139-3141.

Chen, F.W., 2004: Global Estimation of Precipitation Using Opaque Microwave Bands. Ph.D. thesis, Massachusetts Institute of Technology, Department of Electrical Engineering and Computer Science.

Dai, A., F. Giorgi, and K.E. Trenberth, 1999: Observed and Model-Simulated Diurnal Cycles of Precipitation over the Contiguous United States. *Journal of Geophysical Research* (Atmospheres), **104**, 6377-6402.

Negri, A.J., T.L. Bell, and L. Xu, 2002: Sampling of the Diurnal Cycle of Precipitation Using TRMM. *Journal of Atmospheric and Oceanic Technology*, **19**, 1333-1344.

Skofronick-Jackson, G.M., M. Kim, J.A. Weinman, and D. Chang, 2004: A Physical Model to Determine Snowfall over Land by Microwave Radiometry. *IEEE Transactions on Geoscience and Remote Sensing*, **42**, 1047-1058.

Staelin, D.H. and F.W. Chen, 2000: Precipitation Observations near 54 and 183 GHz Using the

NOAA-15 Satellite. *IEEE Trans. Geosci. Remote Sensing*, **38**, 2322-2332**.**

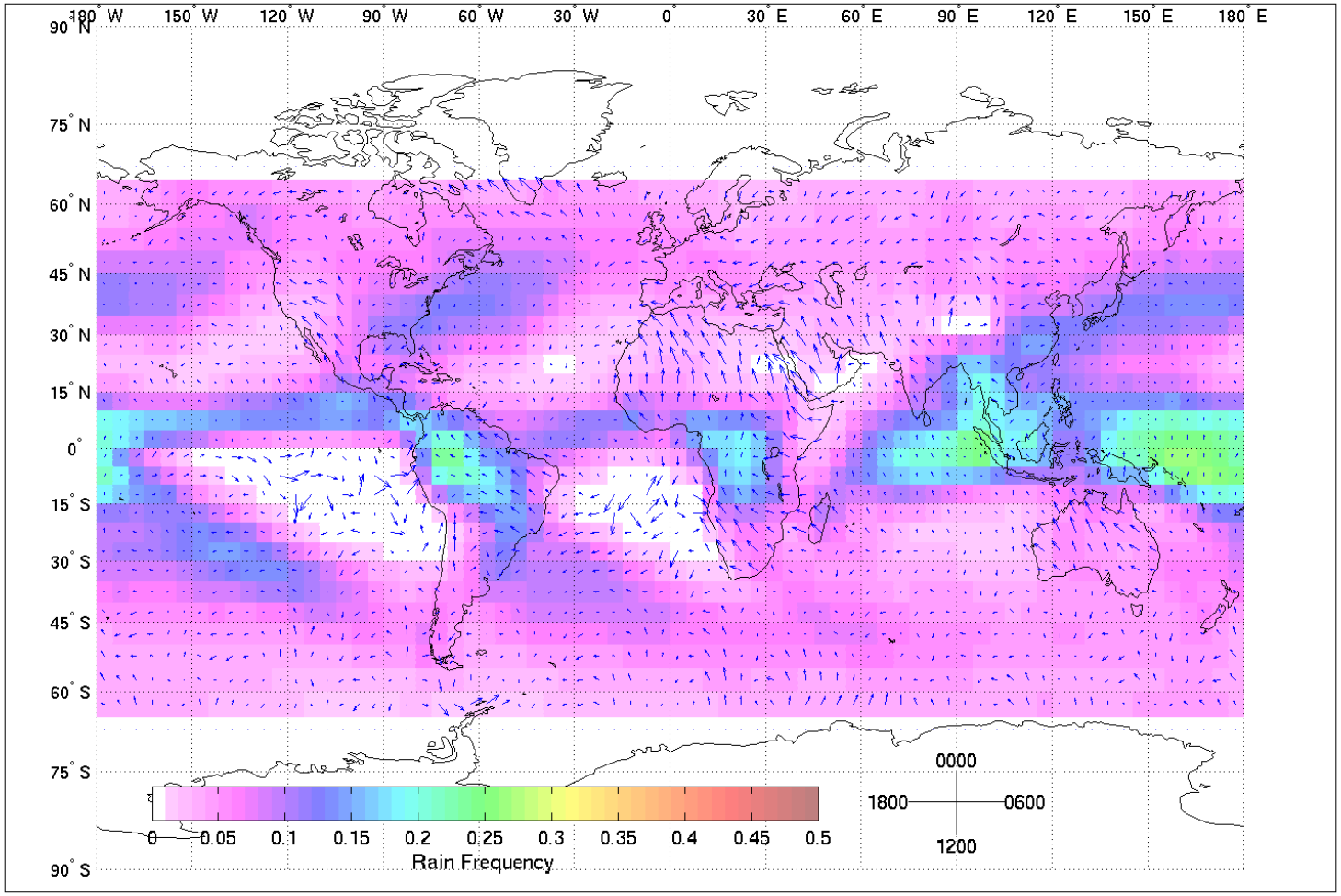

Fig. 5. Diurnal variations of rain frequency from July 2002 to June 2003. Lengths of arrows represent mean-normalized diurnal amplitudes up to 0.5. Directions of arrows represent preferred local times of precipitation.

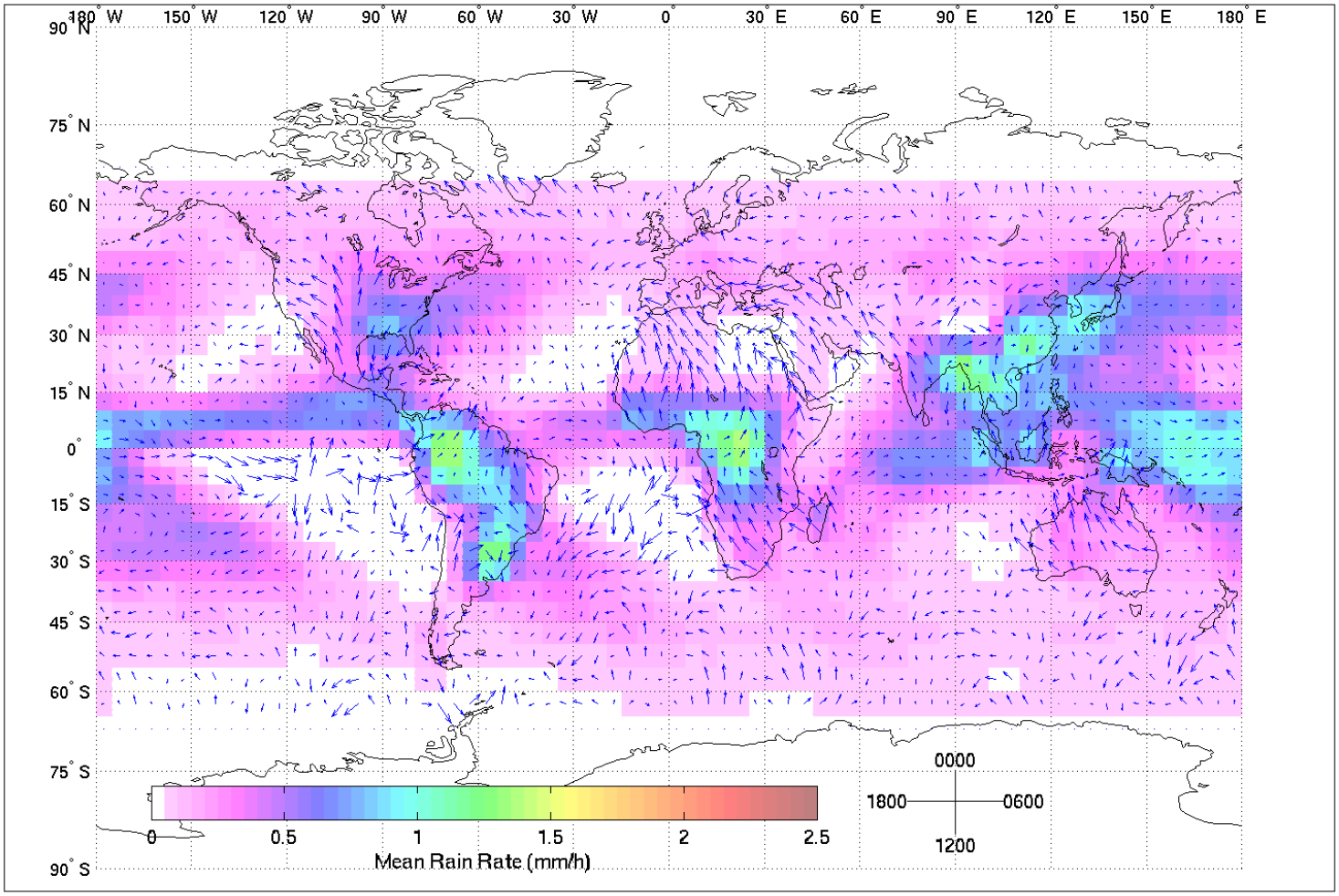

Fig. 6. Diurnal variations of rain rate from July 2002 to June 2003. Lengths of arrows represent mean-normalized diurnal amplitudes up to 0.5. Directions of arrows represent preferred local times of precipitation.